Photopions from nuclei in the distorted-wave impulse approximation

V. Girija

*Department of Nuclear Physics, University of Madras, A.C. College Campus, Madras 600 025, India
and Department of Physics, The Catholic University of America, Washington, D.C. 20064*

V. Devanathan

Department of Nuclear Physics, University of Madras, A.C. College Campus, Madras 600 025, India
(Received 14 December 1981)

The formalism for photoproduction of pions from nuclei has been developed in the distorted-wave impulse approximation, taking into account the effect of the change in pion momentum in nuclear medium. Detailed calculations have been done for the reaction $^{16}O(\gamma,\pi^+)^{16}N$ for photon energies from 170 to 380 MeV, with a view to investigate the effect due to the gradient operator $\vec{\nabla}_\pi$ for momentum of the pion and test the sensitivity of the photopion cross sections to the details of the pion-nucleus optical potential. The results clearly establish that the gradient operator increases the cross sections throughout the energy region considered, the increase being small at lower energies. Also with $\vec{\nabla}_\pi$, the cross sections are rendered less sensitive to the optical potential. The calculated differential cross sections agree very well with the recent experimental data of Shoda *et al.* for γ-ray energy of 200 MeV. However, the cross sections obtained at medium energies are higher when compared to the available experimental data.

> NUCLEAR REACTIONS π^+ photoproduction from ^{16}O; distorted wave impulse approximation; pion-nucleus optical potentials; gradient operator for the pion momentum.

I. INTRODUCTION

The first measurement of the differential cross sections for charged pion photoproduction from ^{10}B and ^{16}O (Ref. 1) in the (3,3) resonance region demands a rigorous and complete study of the reaction. The angular distributions for photon energies up to 200 MeV have been determined by Shoda *et al.*[2] for several nuclei. The photopion cross sections involve three essential ingredients: (i) the elementary amplitude, (ii) the nuclear structure, and (iii) the final state interaction of the pion with the residual nucleus. Among these, the third factor plays a crucial role in such reactions, since the effects due to (a) the interaction of the propagating particle with other nucleons in nuclear medium, (b) the Pauli blocking, and (c) the binding energy which are ignored in the impulse approximation theory, are taken care of by the pion-nucleus optical potential used for the distorted pion. Another important aspect in the study of these reactions lies in the extension of the elementary amplitude to the nuclear problem. Recently, Singham and Tabakin[3] have studied the photopion reactions in light nuclei $6 \leq A \leq 14$ for pion energies from threshold to 150 MeV, using the amplitude of Blomqvist and Laget[4] (BL) which is derived in a general frame. They have introduced the Δ-isobar term in the amplitude and modified the amplitude for coordinate space studies by replacing the momenta of the pion, the initial and final nucleons by their gradient operators. The photoproduction from such light nuclei has also been considered in the framework of distorted wave impulse approximation (DWIA) by Nagl and Überall[5] and Decarlo and Freed.[6] The isobar-doorway approach has been utilized in momentum space for the study of π^0 photoproduction from nuclei by Saharia and Woloshyn.[7] The calculations for the reaction

$$^{16}O(\gamma,\pi^+)^{16}N(J^\pi = 2^-, 0^-, 3^-, 1^-)$$

have been done by us in a previous paper[8] using the asymptotic momentum of the pion in the photopion production amplitude. Earlier, the cross sections

for this reaction had been obtained by Nagl and Überall[9] (NU). Recently, this reaction of π^+ photoproduction from ^{16}O has been studied by Decarlo and Freed.[10] The total cross sections obtained by the three different groups for the four final states of ^{16}N lie below the experimental data of Meyer et al.[11] at medium energies.

The purpose of this paper is to make a systematic and rigorous study of the reaction in DWIA and enable a clear understanding of the process. The formalism is presented in Sec. II in a way suitable for calculations with any of the elementary amplitudes. The calculations have been carried out for the reaction $^{16}O(\gamma,\pi^+)^{16}N$ using the amplitudes of Berends et al.[12] (BDW) and Chew et al.[13] (CGLN). For the final state interaction discussed in Sec. III, the pion-nucleus optical potential of Stricker et al.[14] (SMC) with the Ericson-Ericson correction factor $\xi = 1$ is made use of. The best-fit parameters with $\xi = 0$ obtained by Krell and Barmo[15] (KB) also yield a good fit to the scattering data for pion energies $80-280$ MeV. This potential has also been used in our calculations in order to test the sensitivity of the photoproduction cross sections to the short range behavior of the pion wave functions. The nuclear wave functions that we have utilized in our study are briefly discussed in Sec. IV. The configuration mixing coefficients of Gillet and Vinh Mau[16] and Rho[17] are used in our calculations. These models have been found to reduce the cross sections considerably and the Migdal model with Rho's wave functions yields the correct muon capture rates. In the last section, the results obtained are compared with the available experimental data and the existing theoretical calculations.

II. THE TRANSITION OPERATOR
FOR THE REACTION

The photopion amplitude for nuclear transition from a given initial state to a specified final state is written in the impulse approximation as

$$T = \sum_j t_j = \sum_j \phi^*(\vec{\mu}, \vec{r}_j) t_s(j) \exp(i\vec{v} \cdot \vec{r}_j) , \qquad (1)$$

where the summation index j runs over the A nucleons. $\phi(\vec{\mu}, \vec{r})$ is the distorted pion wave function with asymptotic momentum $\vec{\mu}$ that takes care of the interaction of the pion with the residual nucleus. The incident photon of momentum $\vec{v}$ is represented by a plane wave. $\vec{\mu}$ and $\vec{v}$ represent the momenta

in the laboratory system.

The elementary photopion production amplitude, denoted by t_s in Eq. (1), has the general structure

$$t_s = c\{c_1(\vec{\sigma} \cdot \vec{v})(\vec{\mu} \cdot \vec{\epsilon}) + c_2(\vec{\sigma} \cdot \vec{\epsilon})(\vec{\mu} \cdot \vec{v})$$
$$+ c_3(\vec{\sigma} \cdot \vec{\epsilon}) + c_4(\vec{\sigma} \cdot \vec{\mu})(\vec{\mu} \cdot \vec{\epsilon})$$
$$+ c_5(\vec{\mu} \cdot \vec{v} \times \vec{\epsilon})\} , \qquad (2)$$

where $\vec{\epsilon}$ is the polarization vector of the photon. Only the quantities c, c_1, c_2, c_3, c_4, and c_5 are defined differently in the case of BDW and CGLN amplitudes. $\vec{\mu}$ and $\vec{v}$ are unit vectors in the case of BDW amplitude and

$$c = \frac{2\pi}{(\mu_0 v_0)^{1/2}} , \quad c_1 = F_2 + F_3 ,$$
$$c_2 = -F_2, \quad c_3 = F_1 , \qquad (3)$$
$$c_4 = F_4, \text{ and } c_5 = F_2 .$$

The amplitudes F_i can be decomposed into electric and magnetic multipoles. Retaining those multipoles which possibly contribute for photon energies up to 380 MeV, we obtain

$$F_1 = E_{0+} + P_2'(E_{1+} + M_{1+} + E_{3-} + 4M_{3-})$$
$$+ P_3'(E_{2+} + 2M_{2+}) + E_{2-} + 3M_{2-}$$
$$+ P_4'(E_{3+} + 3M_{3+}) ,$$

$$F_2 = 2M_{1+} + M_{1-} + P_2'(3M_{2+} + 2M_{2-})$$
$$+ P_3'(4M_{3+} + 3M_{3-}) , \qquad (4)$$

$$F_3 = P_2''(E_{1+} - M_{1+} + E_{3-} + M_{3-})$$
$$+ P_3''(E_{2+} - M_{2+}) + P_4''(E_{3+} - M_{3+}) ,$$

$$F_4 = P_2''(M_{2+} - M_{2-} - E_{2+} - E_{2-})$$
$$+ P_3''(M_{3+} - M_{3-} - E_{3+} - E_{3-}) .$$

The individual multipoles including isospin are tabulated by Berends et al.[12] P_l, P_l', and P_l'' are the Legendre polynomials of the first kind and their first and second derivatives. In the case of the CGLN amplitude, the corresponding quantities for positive pion photoproduction are given by

$$c = \frac{2\sqrt{2}\pi e f}{(\mu_0 \nu_0)^{1/2}} \, ,$$

$$c_1 = \lambda h^{--} - \alpha + \frac{2}{1 + \frac{\mu_0}{M}} \frac{1}{k^2 + 1} \, ,$$

$$c_2 = -\lambda h^{--} + \alpha, \quad c_3 = \frac{1}{1 + \frac{\mu_0}{M}} - \alpha \mu_0^2 \, ,$$

$$c_4 = -\frac{2}{\left[1 + \frac{\mu_0}{M}\right](k^2 + 1)} \, ,$$

and

$$c_5 = \lambda h^{-+} \, , \tag{5}$$

with

$$\alpha = \frac{g_p + g_n}{2M\mu_0} \, .$$

k represents the momentum transfer to the target nucleon and μ_0 and ν_0 are the energies of the outgoing pion and photon, respectively. All the other quantities are defined in Ref. 13. We have made sure that the single nucleon cross sections are reproduced with either of the amplitudes, which is a necessary although not a sufficient test for application to nuclear problems. The kinematical variables $\vec{\mu}$, $\vec{\nu}$, μ_0, ν_0, and k occurring in the expression for t_s are in the center of mass system of the pion-nucleon. We take into account the differences in the definitions of the S matrix and also we Lorentz-transform these amplitudes to the laboratory system following Kisslinger.[18]

We now expand the photon and pion wave functions into partial waves.

$$\exp(i\vec{\nu}\cdot\vec{r}) = 4\pi \sum_{l_\nu} (i)^{l_\nu} j_{l_\nu}(\nu r)$$

$$\times \sum_{m_\nu} Y_{l_\nu}^{m_\nu}(\hat{r}) Y_{l_\nu}^{m_\nu *}(\hat{\nu}) \, . \tag{6}$$

$$\phi(\vec{\mu},\vec{r}) = 4\pi \sum_{l_\mu} (i)^{l_\mu} g_{l_\mu}(\mu r)$$

$$\times \sum_{m_\mu} Y_{l_\mu}^{m_\mu}(\hat{r}) Y_{l_u}^{m_\mu *}(\hat{\mu}) \, . \tag{7}$$

$g_{l_\mu}(\mu r)$ is the radial part of the pion wave function, obtained in the usual way by solving the Klein-Gordon equation. In the limit when the distortion goes to zero, $g_{l_\mu}(\mu r)$ goes over into $j_{l_\mu}(\mu r)$ and we can write the transition amplitude in the simplified form

$$t_j = t_s(j)\exp(i\vec{k}\cdot\vec{r}_j) \tag{8}$$

with

$$\vec{k} = \vec{\nu} - \vec{\mu} \, .$$

The closed expression that we obtain in this case can be used to check the correctness of the DWIA program written for the purpose. This also helps to decide the number of partial waves that are to be included for convergence.

Replacing the pion momentum by the gradient operator $\vec{\nabla}_\pi$ and making use of the familiar relation

$$\vec{\nabla}_\pi Y_{l_\mu}^{m_\mu}(\hat{r}) g_{l_\mu}(\mu r) = \sum_L C(l_\mu 1 L, m_\mu \lambda M_\mu) \frac{Y_L^{M_\mu}(\hat{r})}{[L]} \{ \sqrt{L} D_-(l_\mu) g_{l_\mu}(\mu r) \delta_{L, l_\mu + 1}$$

$$- \sqrt{L+1} D_+(l_\mu) g_{l_\mu}(\mu r) \delta_{L, l_\mu - 1} \} \, , \tag{9}$$

with

$$D_-(l_\mu) = \left[\frac{d}{dr} - \frac{l_\mu}{r}\right] g_{l_\mu}(\mu r)$$

and

$$D_+(l_\mu) = \left[\frac{d}{dr} + \frac{l_\mu + 1}{r}\right] g_{l_\mu}(\mu r) \, ,$$

we arrive at the following expression for the transition operator using Eqs. (1), (2), (6), (7), and (9):

$$
t_j = (4\pi)^{3/2} \sum_{l_\mu,l_\nu} (i)^{l_\nu - l_\mu} [l_\nu] \sum_{L,L_T,\mathscr{L}} \frac{1}{[L_T]} C(\mathscr{L}l_\nu L_T, 000)
$$

$$
\times \sum_{M_\lambda} (-1)^{M_\lambda} \sum_{K,L_1,L_2} [\{(\nu_K \times \epsilon)_{L_2} \times Y_{l_\mu}(\hat{\mu})\}_{L_1} \times Y_{l_\nu}(\hat{\nu})]_\lambda^{-M_\lambda}
$$

$$
\times \sum_n (Y_{L_T}(\hat{r}_j) \times \sigma_n(j))_\lambda^{M_\lambda}
$$

$$
\times \Big[\delta_{n,1}\delta_{\mathscr{L},L} W(1L\lambda l_\nu, L_1 L_T)
$$

$$
\times (\delta_{K,1}[-W(K1L_1 l_\mu, L_2 L)[L_1][L_T][L_2][L]
$$

$$
\times \{c_1 + (-1)^{L_2} c_2\} R_1(l_\mu, L, r_j)]
$$

$$
+ \delta_{K,0}[\delta_{L_2,1}
$$

$$
\times \{ \delta_{L,l_\mu}\delta_{\mathscr{L},L} ic_3 [L_1][L_T][L] g_{l_\mu}^*(\mu r_j) j_{l_\nu}(\nu r_j)
$$

$$
+ \delta_{L_1,L} ic_4 [L_T] R_2(l_\mu, L, \mathscr{L}, r_j)\}])
$$

$$
+ \delta_{n,0}\delta_{K,1}\delta_{\mathscr{L},L}\delta_{L_2,1}\delta_{L_1,L}\delta_{\lambda,L_T}\sqrt{2}c_5 \times R_1(l_\mu, L, r_j) \Big] \tag{10}
$$

with $\sigma_0 = 1$, $\sigma_1 = \vec{\sigma}$, $\nu_0 = 1$, and $\nu_1 = \vec{\nu}$.

The summation indices over n and K can take only two values 0 and 1. R_1 and R_2 are the radial integrals which involve the derivatives of the pion wave functions, given by

$$
R_1(l_\mu, L, r_j) = \{\sqrt{L}(D_-(l_\mu)g_{l_\mu}(\mu r_j))^* \delta_{L,l_\mu+1} - \sqrt{L+1}(D_+(l_\mu)g_{l_\mu}(\mu r_j))^* \delta_{L,l_\mu-1}\} j_{l_\nu}(\nu r_j)
$$

and

$$
R_2(l_\mu, L, \mathscr{L}, r_j) = \{\sqrt{L}\delta_{L,l_\mu+1}[\sqrt{\mathscr{L}}\{D_-(l_\mu+1)D_-(l_\mu)g_{l_\mu}(\mu r_j)\}^* \delta_{\mathscr{L},L+1}
$$

$$
- \sqrt{\mathscr{L}+1}\{D_+(l_\mu+1)D_-(l_\mu)g_{l_\mu}(\mu r_j)\}^* \delta_{\mathscr{L},L-1}]
$$

$$
- \sqrt{L+1}\delta_{L,l_\mu-1}[\sqrt{\mathscr{L}}\{D_-(l_\mu-1)D_+(l_\mu)g_{l_\mu}(\mu r_j)\}^* \delta_{\mathscr{L},L+1}
$$

$$
- \sqrt{\mathscr{L}+1}\{D_+(l_\mu-1)D_+(l_\mu)g_{l_\mu}(\mu r_j)\}^* \delta_{\mathscr{L},L-1}]\} j_{l_\nu}(\nu r_j) . \tag{11}
$$

Throughout, the symbol $[l]$ denotes $(2l+1)^{1/2}$. For angular momentum coefficients and reduced matrix elements, we follow the notations and conventions of Rose.[19] The transition matrix element, involving a number of summations, need not cause any distress, since for purposes of numerical calculations, seven to eight partial waves are enough to produce convergence for the energy region under consideration. This transition operator is now to be evaluated between the initial and final nuclear states. The matrix element

$$
Q = \langle J_f M_f | T | J_i M_i \rangle \tag{12}
$$

is to be squared thereafter, summed over the final spin states, and averaged over the initial spin states.

The present study does not include the effect of isobar-nucleus dynamics in the photopion production operator. The isobar-doorway model provides the framework for doing so. This approach will be involved for charged pion photoproduction if one

has to do it exactly, preserving the physical nonlocality that arises for the π,N and isobar propagation. The problem becomes simpler for coherent π^0 production, since in this case, the doorway states are the same as those for elastic scattering; it has been studied by Saharia and Woloshyn[7] recently. In the recent DWIA calculation by Singham and Tabakin,[3] the γ-π operator is subjected to distinct medium alteration, whereby the magnetic coupling terms are modified by the Δ-isobar term, introduced by hand in the BL amplitude. It has been stated that the contribution of the isobar to the total cross sections is minimal, caused by the decreasing form factor and pion absorption, and the contribution is less than 25% even at high energies. Hence we feel that it is worthwhile making the DWIA calculation in our present formalism, although it does not include the effects due to isobar dynamics. Further, the amplitudes given by Eq. (2) are written down using the momentum conservation relation in the center of mass frame

$$\vec{p}_i + \vec{v} = \vec{p}_f + \vec{\mu} \ .$$

Singham and Tabakin,[3] in their use of the BL operator, replace the initial and final nucleon momenta $\vec{p}_i$ and $\vec{p}_f$ also by their gradients and use the momentum conservation relation to avoid the momenta occurring in the propagators. With such a treatment, they report that the transition densities that involve the derivatives of the nuclear wave functions are small when compared to those that do not involve the gradients.[3] This is in conformity with our calculations, where we find that the effect of the $(\vec{\sigma}\cdot\vec{\mu})$ $(\vec{\mu}\cdot\vec{\epsilon})$ term in the amplitude is not as significant as the other terms. This also clearly reveals that the gradient operator for the nucleon does not produce significant changes in the cross section.

In the expression for T, there is a clear separation of the factors involving nuclear structure from those that arise due to the production amplitude. This proves to be convenient to study the relative importance of each of the factors in the amplitude, such as the gradient operator $\vec{\nabla}_\pi$ for the pion momentum. This is in contrast to the expression used by other authors (Refs. 3 and 9), wherein the various terms are linked together in the transition operator. The angular momentum operator

$$[Y_L(\hat{r}_j) \times \sigma_n(j)]_\lambda^{M_\lambda}$$

causes the nuclear transition. The only other factor, dependent upon M_λ, is

$$S = [\{(v_K \times \epsilon)_{L_2} \times Y_{l_\mu}(\hat{\mu})\}_{L_1} \times Y_{l_v}(\hat{v})]_\lambda^{-M_\lambda}$$

$$= C(L_1 l_v \lambda, -M_\lambda 0 - M_\lambda)\frac{[l_v]}{(4\pi)^{1/2}}$$

$$\times \sum_{m_1} C(L_2 l_\mu L_1, m_1, -M_\lambda - m_1, -M_\lambda)$$

$$\times Y_{l_\mu}^{-M_\lambda - m_1}(\hat{\mu})C(K1L_2, 0m_1m_1)v_K\epsilon_1^{m_1'}$$

(13)

In the above reduction, the direction of the incident photon is the Z axis. The summations occurring over m_1 and M_λ make the operator t_j independent of the magnetic quantum numbers. It is to be noted that the transition operator is evaluated numerically for a particular m_1 and M_λ and then squared bearing in mind the fact that

$$\epsilon_1^{m_1}\epsilon_1^{m_1'*} = (-1)^{m_1+1}\delta_{m_1,m_1'} \ ,$$

where the primed factor occurs on squaring. The differential cross sections for the process of photoproduction of pions from nuclei is given by

$$\frac{d\sigma}{d\Omega} = (2\pi)^{-2}\mu\mu_0|Q|^2 \ , \tag{14}$$

where μ_0 is the energy of the pion in the laboratory system.

III. THE FINAL STATE INTERACTION

The pion optical wave functions $g_{l_\mu}(\mu r)$ used in the last section must be obtained by solving the wave equation with a suitable pion-nucleus optical potential that can reproduce well the elastic scattering data. This is again a necessary, although not a sufficient condition, since there may exist phase-shift equivalent potentials which may reproduce the scattering data but provide different wave functions in the nuclear interior. It has been shown[20] for ^{12}C that these phase-shift equivalent potentials have just a little effect on the photopion cross sections. Haxton[21] has shown that the apparent sensitivity of the cross sections to the optical potential disappears when one uses realistic potentials.

We solve the modified Klein-Gordon equation

$$\{\nabla^2 + \mu^2\}\psi(\vec{r}) = 2\omega V(r)\psi(\vec{r}) \ , \tag{15}$$

where $\vec{\mu}$ and ω are the momentum and total energy of the pion in the center of mass of the pion-nucleus system. The pion-nucleus interaction is contained in the scalar part of the potential that takes into account the Coulomb effects.

$$2\omega V(r)=q(r)-\vec{\nabla}\cdot\alpha(r)\vec{\nabla}+2\omega V_c(r) \; , \qquad (16)$$

in which the forms for the local and nonlocal parts of the interaction are taken from Stricker et al.[14] (SMC).

$$q(r)=-4\pi\left[p_1\{\bar{b}_0\rho(r)-b_1(\rho_n(r)-\rho_p(r))\} \right.$$

$$+p_2 B_0\rho^2(r)+\frac{(p_1-1)}{2}\nabla^2 c(r)$$

$$\left. +\frac{C_0(p_2-1)}{2p_2}\nabla^2\rho^2(r) \right]$$

and

$$\alpha(r)=-4\pi\left[\frac{c(r)}{1+\dfrac{4\pi\xi}{3}\dfrac{(A-1)}{A}c(r)}+\frac{C_0}{p_2}\rho^2(r) \right] \; ,$$

$$(17)$$

in which $\alpha(r)$ is made less attractive by the Ericson-Ericson factor that arises due to the polarization of the p-wave pion field. The extent to which the attraction is weakened is determined by the parameter ξ. The pion-nucleus optical potential defined by Eq. (16) takes into account the multiple scattering effects. The terms $\nabla^2 c\rho(r)$ and $\nabla^2 C_0\rho^2(r)$ that also stem from the π-N p-wave scattering, arise out of the angle transformation of the $(\vec{\mu}\cdot\vec{\mu}\,')$ factor and increase the cross sections at the backward angles for low energy pions. It has been shown that these terms have a negligible effect on the cross sections at medium energies.[22]

As one approaches the resonance region, a fairly good fit to the scattering data can be obtained by varying the dominant p-wave parameter $c_0(r)$ that is contained in $c(r)$ and assuming reasonable values for other parameters. Setting $\xi=0$ and $V_c=0$, Krell and Barmo (KB) have obtained a fit to the scattering data for 80−280 MeV pions. We also make use of their parameters redefining $q(r)$ and $\alpha(r)$ accordingly, to facilitate a comparative study.
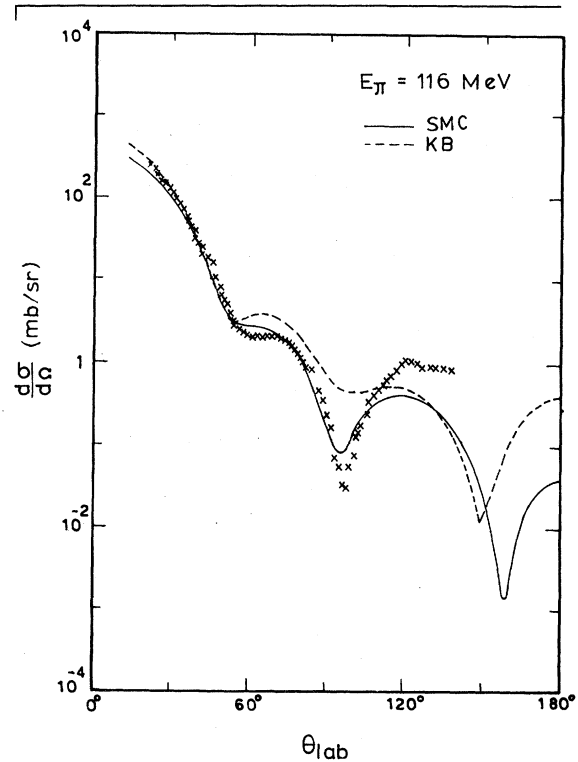
We require the solution of the radial equation

$$\left[\frac{d^2}{dr^2}-\frac{l(l+1)}{r^2}-\frac{1}{1+\alpha(r)}\left\{ \frac{\alpha'(r)}{r}+\frac{\alpha''(r)}{2}-\frac{[\alpha'(r)]^2}{4(1+\alpha(r))}-\beta(r)+2\omega V_c(r) \right\} \right]\tilde{u}_l(r)=0 \; , \qquad (18)$$

where

$$\beta(r)=\mu^2-q(r) \; .$$

The transformed wave functions $\tilde{u}_l(r)$ are related to the g_l's that are required for the distorted wave theory in the following way:

$$u_l(r)=\frac{\tilde{u}_l(r)}{(1+\alpha(r))^{1/2}}=\mu r g_l(\mu r) \; . \qquad (19)$$

When $V(r)\rightarrow 0$, we have

$$u_l(r)\rightarrow\tilde{u}_l(r)\rightarrow\mu r j_l(\mu r) \; . \qquad (20)$$

The partial waves of the pions, which are denoted by l in this section, were denoted by l_μ in Sec. II.

Stricker et al. have obtained good fits to the scattering data for π^+ ^{16}O for low energies of the pion. The elastic scattering cross sections obtained with the two sets of parameters SMC and KB for pion energies of 116 and 170 MeV are shown in Figs. 1 and 2. The SMC parameters, providing a more refined potential, show a better fit to the data of Albanese et al.[23] There is also a change in the position of the first minima, resulting from the different strengths of the s and p wave amplitudes. The real and imaginary parts of the wave functions obtained with the two potentials are shown in Figs. 3 and 4 for the same pion energies. The wave functions depict an increase in absorption in the nuclear

FIG. 1. Elastic scattering of positive pions on ^{16}O for laboratory energy of the pion $E_\pi=116$ MeV, compared with the experimental data of Albanese et al. (Ref. 23). The continuous and dashed curves are obtained by using the SMC and KB potentials, respectively.
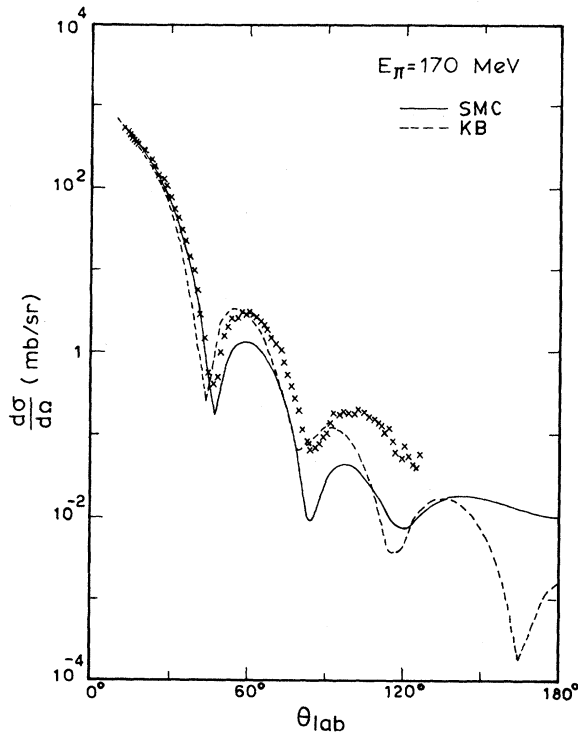
FIG. 2. Elastic scattering of π^+ by ^{16}O. Experimental data (Ref. 23) are for 163 MeV.

region, as one approaches resonance. The SMC potential has a tendency to decrease the amount of absorption, as illustrated by the real parts of the wave functions [and $|u_l(r)|$ which are not shown]. This is reflected in turn in the photopion cross sections that show an increase. The wave functions, used for the distorted pions, are those of π^+ ^{16}N which show a similar behavior.
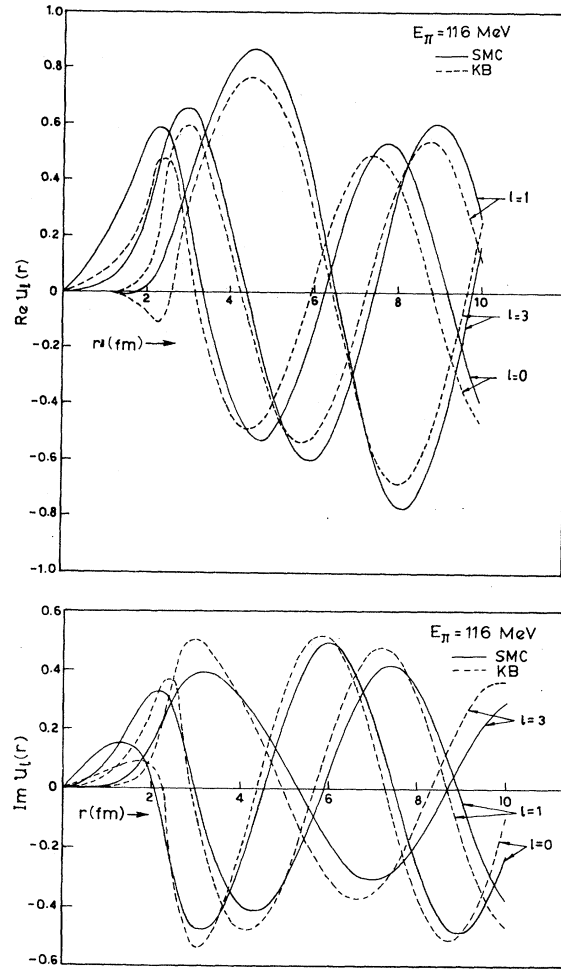

FIG. 3. Distorted pion wave functions for the various pion partial waves for laboratory pion energy of 116 MeV. (a) Real parts of the wave functions and (b) imaginary parts of the wave functions.

IV. NUCLEAR WAVE FUNCTIONS

The bound state wave functions generated with the Woods-Saxon potential have been used in the independent particle model in our previous calculations[8] for ^{16}O and have been shown to yield large cross sections. The necessity for utilizing the configuration mixing model has also been stressed by Devanathan et al.[24] It has been shown that the photopion cross sections are not affected to any

great extent by the short range correlations.[25] In this paper, we have used the admixture of the wave functions using the coefficients of Gillet and Vinh Mau (GV). This again overestimates the cross sections. Rho's wave functions, obtained from Migdal's theory for the low excited states by fitting the static moments and transition moments, are found to yield the experimentally evaluated muon capture rates, and hence we use these wave functions in our present study.

$$|J_fM_f\rangle = \sum_{\substack{p,h \\ m_p,m_h}} X_{p,h}^{J_f} C(j_pj_hJ_f, m_p - m_hM_f)(-1)^{j_h-m_h} a_{j_p,m_p}^\dagger a_{j_h,m_h} |0\rangle , \tag{21}$$
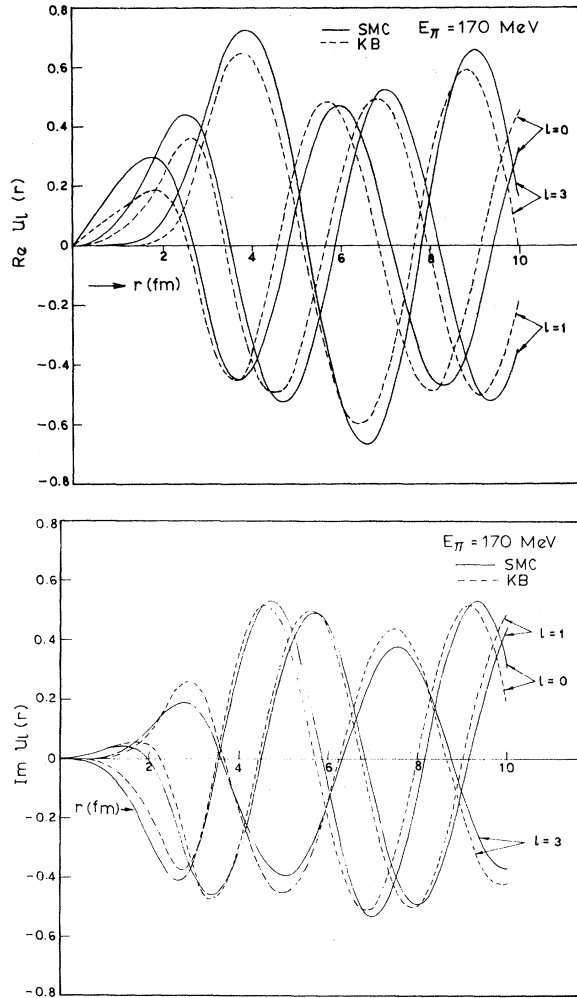
FIG. 4. The pion optical wave functions for laboratory pion energy of 170 MeV. (a) The real parts and (b) the imaginary parts.

where $X^{J_f}_{p,h}$ are the configuration mixing coefficients satisfying the usual normalization and $|0\rangle$ is the Hartree-Fock ground state.

V. RESULTS AND DISCUSSION

Detailed numerical calculations have been done for the reaction $^{16}O(\gamma,\pi^+)^{16}N(2^-,0^-,3^-,1^-)$ using (i) the gradient operator $\vec{\nabla}_\pi$ for the pion momentum and (ii) the asymptotic momentum of the pion for laboratory photon energies (E_γ) from 170 to 380 MeV. This is with a view to study the effect of $\vec{\nabla}_\pi$ on the photopion cross sections. The sensitivity of the cross sections to the pion-nucleus optical potential is studied by using the SMC (with $\xi=1$) and KB (with $\xi=0$) potentials. In both cases, the
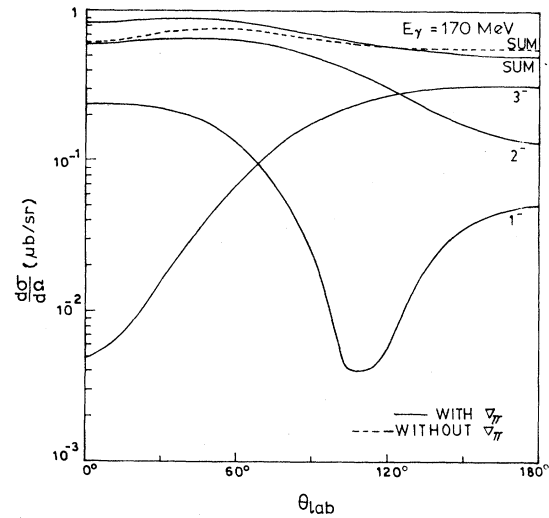

FIG. 5. Angular distribution for the reaction $^{16}O(\gamma,\pi^+)^{16}N$ for laboratory photon energy of 170 MeV. Sum denotes the sum of the cross sections obtained for the four final states of ^{16}N (2^-, 0^-, 3^-, and 1^-). The cross sections for the 0^- transition are small and hence not shown.

parameters have been interpolated as and when necessary. Numerical calculations have been carried out with (i) the BDW amplitude which does not involve the pion momentum in an inconvenient way and (ii) the CGLN amplitude using the dominant δ_{33} phase shift. As a first step, the codes written in DWIA with and without $\vec{\nabla}_\pi$ have been
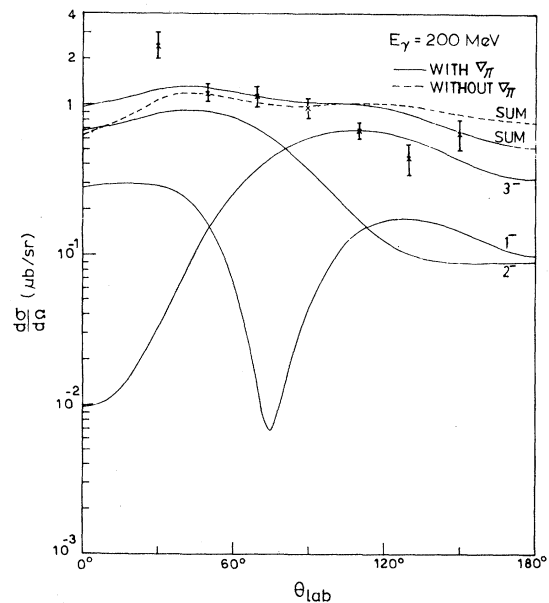

FIG. 6. Angular distribution for γ-ray energy 200 MeV compared with the data of Shoda et al.[2] See caption of Fig. 5 for other details.
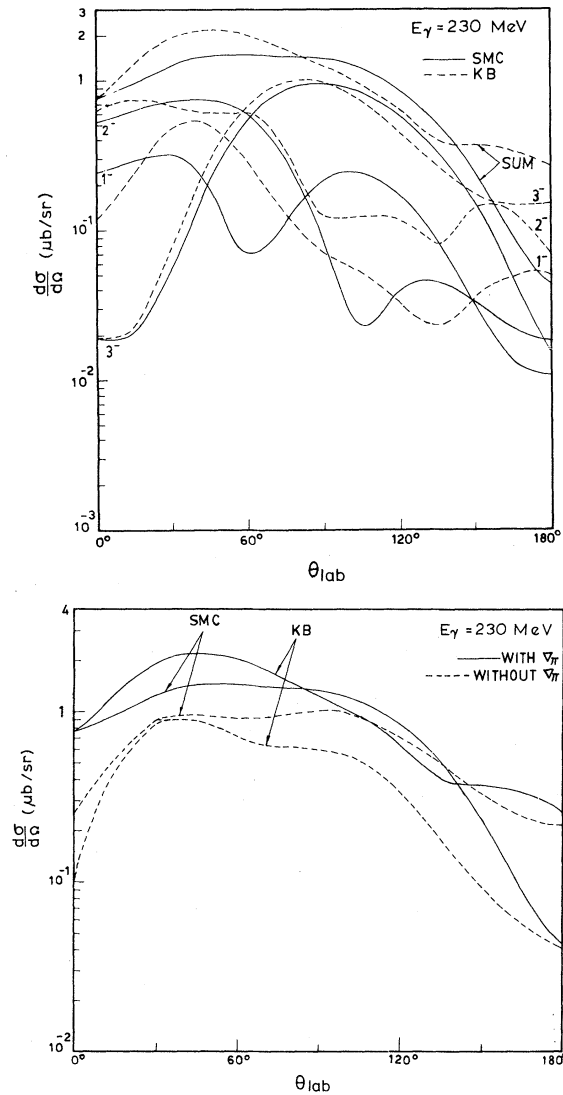
FIG. 7. Differential cross sections for π^+ photoproduction from ^{16}O. (a) The results obtained with $\vec{\nabla}_\pi$ to discrete final states of ^{16}N. Sum denotes the sum of the cross sections obtained for the four final states of ^{16}N. (b) Sum of the cross sections obtained for the states 2^-, 0^-, 3^-, and 1^- of ^{16}N.

checked up thoroughly in the limit of the distortion going to zero. Rho's wave functions are used in all the calculations, unless otherwise stated.

The angular distributions obtained for the incident γ ray of energies 170 and 200 MeV with the BDW amplitude are shown in Figs. 5 and 6. The effect of $\vec{\nabla}_\pi$ is to increase the cross sections at the forward angles, and to decrease them at the backward angles, thereby yielding a better agreement with the recent experiment of Shoda et al.[2] at 200 MeV. The effect of $\vec{\nabla}_\pi$ is, however, small due to the dominance of the $(\vec{\sigma}\cdot\vec{\epsilon})$ term in the amplitude
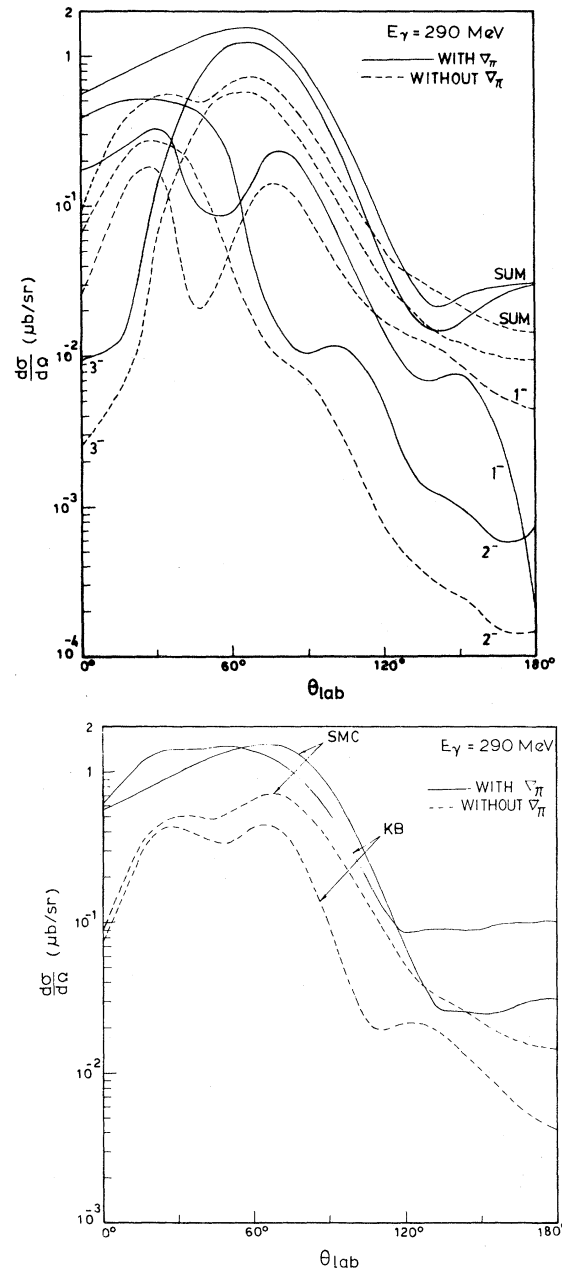

FIG. 8. Differential cross sections for $E_\gamma = 290$ MeV. (a) Cross sections to discrete final states of ^{16}N and the sum of the cross sections for the four final states of ^{16}N, obtained with the SMC potential. (b) Sum of the cross sections for the four final states of ^{16}N.

at these energies.

Figures 7−9 depict the angular distributions for photon energies 230, 290, and 350 MeV arrived at by using the BDW amplitude. Comparing the results plotted in Figs. 7(b)−9, it is found that the effect of $\vec{\nabla}_\pi$ is to increase the cross sections considerably at the forward angles, with an overall increase
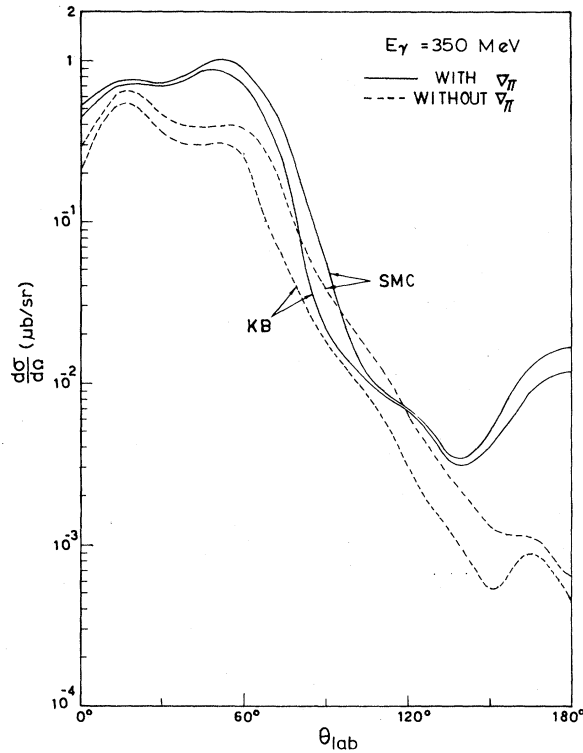
FIG. 9. Cross sections summed over the four final states of ^{16}N.

in the integrated cross sections, when the SMC potential is used in the calculations. With the KB potential, the $\vec{\nabla}_\pi$ increases the cross sections at all angles. This is revealed by Figs. 7(b), 8(b), and 9. The sensitivity of the cross sections to the pion-nucleus optical potential is shown in Figs. 7(a), 7(b), 8(b), and 9. With $\vec{\nabla}_\pi$, the KB potential increases the cross sections at the forward angles, decreases them at the mid angles, and again provides an increase at the backward angles at 230 and 290 MeV. The cross sections with the SMC potential parameters are higher throughout for all angles for photon energy 350 MeV. These changes are about 40% at 230 MeV, decreasing as one goes to higher energies. A similar result has been obtained by Singham and Tabakin[3] for the case of π^+ and π^- photoproduction from ^{14}N. Figures 7(b), 8(b), and 9 reveal that employing the asymptotic momentum, the SMC potential increases the cross sections for all angles. These three figures also support the fact that without $\vec{\nabla}_\pi$, the cross sections become much more sensitive to the pion-nucleus optical potential. The same information can be had by looking at Figs. 10 and 11, again obtained with the BDW amplitude, wherein our results are compared with the experimental data of the MIT group.[1]
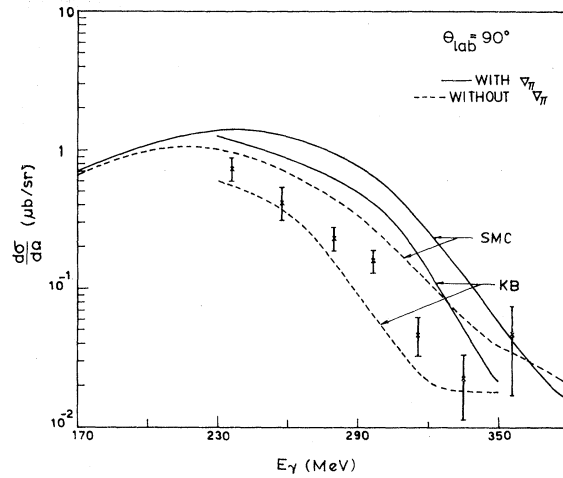

FIG. 10. The differential cross sections at 90° as a function of gamma energy. The contributions from all the four low lying final states of ^{16}N are included and compared with the data of Bosted et al.[1]

Figure 12 depicts the total cross sections obtained in the plane wave impulse approximation (PWIA) and DWIA. The curve g is obtained with the CGLN amplitude and all other curves are derived with the BDW amplitude. For photon energies 170 and 200 MeV, the final state interaction contributes very little and the $(\vec{\sigma} \cdot \vec{\epsilon})$ term in the amplitude is dominant. Hence, the nuclear structure plays a major role in the determination of the cross sections at these energies. At medium energies, with the reliable pion-nucleus optical potential (SMC) and the Migdal wave functions, the cross sections obtained with $\vec{\nabla}_\pi$ are higher, and without $\vec{\nabla}_\pi$, are lower when compared to the experimental data of Meyer et al.[11]
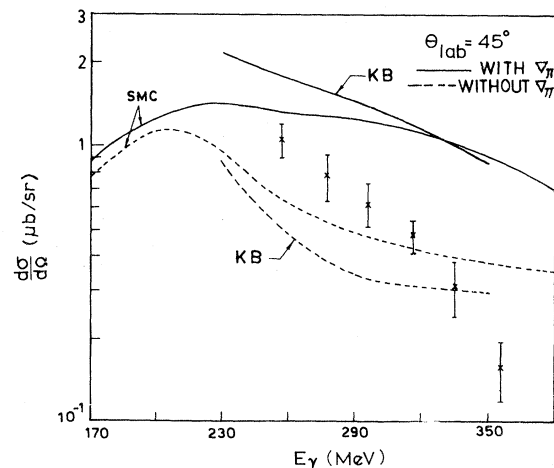

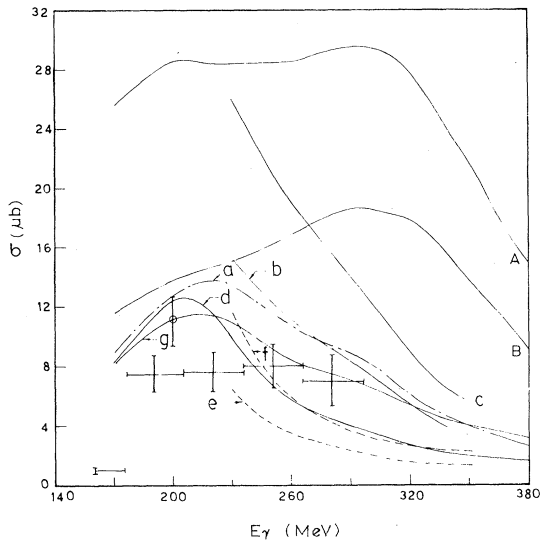FIG. 11. Differential cross sections at 45°. See caption of Fig. 10 for other details.

FIG. 12. The total cross sections summed over the four final states of ^{16}N. A and B are obtained in PWIA. The curves, a, b, c, and g are obtained with $\vec{\nabla}_\pi$ and d, e, and f without $\vec{\nabla}_\pi$. The SMC potential is used for curves a, d, and g and b, c, e, and f are obtained with the KB potential. Curves A, c, and f correspond to GV wave functions and the others to Rho's wave functions. The curve g is obtained with the CGLN amplitude and the rest with the BDW amplitude. Experimental data are from Ref. 11. The experimental point Φ corresponds to the results of Shoda et al.[2]

The total cross sections for the four discrete states of ^{16}N obtained with and without $\vec{\nabla}_\pi$ using the SMC and KB potentials are displayed in Table I. The following observations can be made, by looking at the sum of the cross sections for the four final states of ^{16}N:

(i) The $\vec{\nabla}_\pi$ increases the total cross sections by about $50-60\%$ with the SMC potential at medium energies. The increase in the results with $\vec{\nabla}_\pi$ is much more (i.e., by a factor of $2-3$) when one employs the KB potential.

(ii) The SMC potential when compared to the potential of Krell and Barmo decreases the cross sections for photon energies 230 and 260 MeV and increases the cross sections for energies $290-350$ MeV. This is observed when one uses a refined amplitude (with $\vec{\nabla}_\pi$) and these changes are about 15% at 230 MeV but only 3 to 5% from $260-350$ MeV. Using the asymptotic momentum of the pion, the SMC potential uniformly increases the cross sections at all energies from $230-350$ MeV, the increase being 50% at 230 MeV, falling to about 20 to 30% between $260-350$ MeV. In short, employing

$\vec{\nabla}_\pi$, the sensitivity of the cross sections to the potential decreases and it may be much less, if one uses realistic phase-shift equivalent potentials, in conformity with the results of Haxton.[21] However, the differential cross sections change appreciably with the two potentials, even with $\vec{\nabla}_\pi$, as stated earlier.

(iii) Comparing the cross sections obtained with the BDW and the CGLN amplitudes, it is found that the total cross sections obtained with the CGLN amplitude are lower up to 320 MeV and slightly higher for 350 and 380 MeV. The differences are about 10 to 20% and they are attributed to the neglect of the other p-wave phase shifts in the CGLN amplitude since we find that the changes are minimal near the 3-3 resonance.

(iv) The cross sections obtained with the BDW amplitude, the gradient operator $\vec{\nabla}_\pi$, the SMC potential, and the Migdal wave functions exactly reproduce the shape of the data of Meyer et al.[11] and are in good agreement when we scale by a factor of $\frac{2}{3}$ (Fig. 13).

To compare our results with the other two available calculations, we bear in mind that the work of DeCarlo and Freed[10] (DF) employs the asymptotic momentum for the pion and the nuclear wave functions of Donnelly and his co-workers, and that of Nagl and Überall[9] (NU) uses the gradient operator $\vec{\nabla}_\pi$ and the Helm model wave functions. Our results with the asymptotic momentum of the pion compare favorably well with the DF calculations and both these provide quite a good fit to the data of the MIT group[1] for the pion emission angle of 90°. The two calculations are in excellent agreement with the recent angular distribution data of the Tohoku group[2] for $E_\gamma = 200$ MeV but lie below the total cross section data of Meyer et al.[11] With $\vec{\nabla}_\pi$, we obtain cross sections which are 1.5 times higher than the results of Meyer et al. It is surprising that the calculations of NU agree with the cross sections of Meyer et al. for $E_\gamma = 200$ MeV, and are thereby lower by a factor of 1.5 when compared to the experiment of Shoda et al.[2] and the other two calculations. The agreement between our calculations and those of DF are in support of the fact that both of us have used wave functions which explain the transverse electron scattering form factor,[17] β decay, and muon capture. Further, a calculation of the transition densities with the Helm model and Migdal wave functions reveals that the former provides lower transition densities. There is a significant crossing of the total cross section curve of NU with our two curves (obtained with the asymptotic momentum for the pion) at about 250 MeV of the

TABLE I. Cross sections for the reaction $^{16}O(\gamma,\pi^+)^{16}N$ obtained with the Midgal wave functions. The sum denotes the sum of cross sections to all the four states 0^-, 1^-, 2^-, and 3^-.

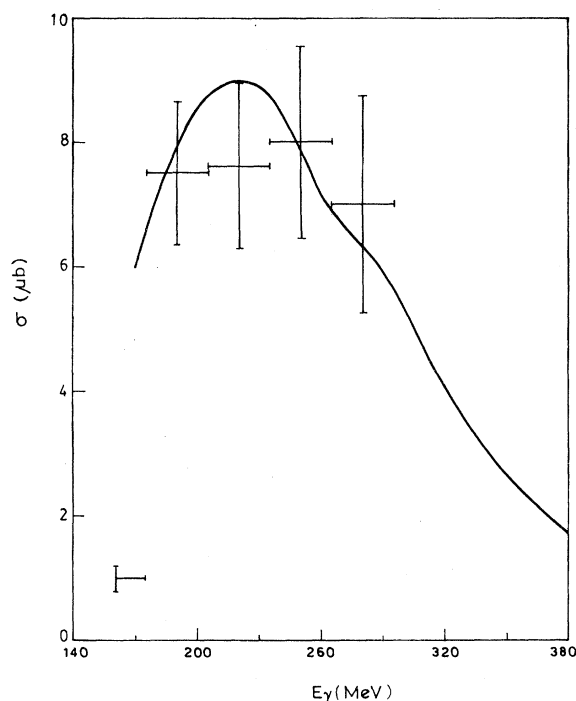| γ-ray energy (MeV)	^{16}N state	BDW,SMC (with $\vec{\nabla}_\pi$)	BDW,KB (with $\vec{\nabla}_\pi$)	BDW,SMC (without $\vec{\nabla}_\pi$)	BDW,KB (without $\vec{\nabla}_\pi$)	CGLN,SMC (with $\vec{\nabla}_\pi$)
			Cross section in μb			
170	0^-	0.041		0.006		0.072
	1^-	0.939		1.031		0.902
	2^-	5.833		4.828		5.290
	3^-	2.157		2.432		1.944
	Sum	8.970		8.297		8.208
200	0^-	0.326		0.025		0.451
	1^-	1.564		1.645		1.435
	2^-	5.602		5.126		4.482
	3^-	5.307		5.686		4.826
	Sum	12.799		12.482		11.194
230	0^-	1.291	2.826	0.102	0.125	2.006
	1^-	1.983	2.009	1.670	1.134	1.683
	2^-	3.385	3.759	2.738	1.646	2.034
	3^-	6.696	6.743	5.339	3.573	5.294
	Sum	13.355	15.337	9.849	6.478	11.017
260	0^-	0.800	1.110	0.114	0.078	1.612
	1^-	1.533	1.590	1.016	0.640	1.171
	2^-	2.155	2.586	1.077	0.609	1.501
	3^-	6.220	5.829	3.480	2.171	4.088
	Sum	10.708	11.115	5.687	3.498	8.372
290	0^-	0.395	0.465	0.127	0.069	0.816
	1^-	1.347	1.209	0.736	0.398	1.111
	2^-	1.476	1.733	0.583	0.307	1.236
	3^-	5.623	4.947	2.591	1.490	3.932
	Sum	8.841	8.354	4.037	2.264	7.095
320	0^-	0.187	0.200	0.114	0.075	0.298
	1^-	0.942	0.762	0.482	0.275	0.922
	2^-	0.998	1.030	0.428	0.255	1.039
	3^-	3.900	3.283	1.648	1.012	3.087
	Sum	6.027	5.275	2.672	1.617	5.346
350	0^-	0.122	0.122	0.097	0.077	0.165
	1^-	0.635	0.497	0.352	0.241	0.727
	2^-	0.721	0.669	0.405	0.277	0.939
	3^-	2.481	2.046	1.091	0.753	2.224
	Sum	3.959	3.334	1.945	1.348	4.055
380	0^-	0.083		0.079		0.121
	1^-	0.456		0.309		0.601
	2^-	0.540		0.409		0.867
	3^-	1.517		0.804		1.604
	Sum	2.596		1.601		3.193

FIG. 13. Sum of the total cross sections for the four final states of ^{16}N obtained with the BDW amplitude, the operator $\vec{\nabla}_\pi$, the SMC potential, and the Migdal wave functions, scaled by a factor of $\frac{2}{3}$, are compared with the data of Meyer *et al.* (Ref. 11).

photon energy. This may be due to the Helm model parametrization with the $(\vec{\sigma} \cdot \vec{\epsilon})$ term developing uncertainties because of the increasingly strong dependence of the cross sections on the pion momentum-dependent terms. Furthermore, there is no unique way of fitting the Helm model parameters to the electron scattering form factor since the four states are being summed over.

VI. CONCLUSION

The present study of the reaction $^{16}O(\gamma,\pi^+)^{16}N$ clearly indicates that the effect of the gradient operator for the pion momentum is to increase the cross sections considerably at medium energies. Also, it is found that the sensitivity of the photopion cross sections to the pion-nucleus optical potential decreases by employing a refined DWIA approach and it may decrease still further if one uses realistic phase-shift equivalent potentials.

Among the calculations reported, we feel that the cross sections obtained by using the gradient operator $\vec{\nabla}_\pi$, the SMC potential, and the Migdal wave functions are the most reliable. The results obtained with these are in excellent agreement with the recent angular distribution data of the Tohoku group[2] for photon energy of 200 MeV. Our calculations with the asymptotic momentum of the pion agree better with the differential cross section measurements of the MIT group for medium energies of the photon. It is surprising that with refinements, the agreement has become poorer and the present calculations are somewhat larger than the MIT data. Also it is noticed that the calculated total cross sections reported here are 1.5 times larger than the old data of Meyer *et al.* Since there has been increasing experimental activity for this reaction,[26] we can look forward to more reliable data in the near future to enable us to come to a definite conclusion.

ACKNOWLEDGMENTS

[1]P. E. Bosted *et al.*, Phys. Rev. Lett. 45, 1544 (1980); P. E. Bosted, Ph.D. dissertation, Massachussetts Institute of Technology, 1980.

[2]K. Shoda, private communication; M. Yamazaki *et al.*, abstracts of contributed papers to the IX International Conference on High Energy Physics and Nuclear Structure, Versailles, 1981, p. 115.

[3]M. K. Singham and F. Tabakin, Ann. Phys. (N.Y.) 135, 71 (1981); F. Tabakin, *Photopion Nuclear Physics* (Plenum, New York, 1979), p. 301.

[4]I. Blomqvist and J. M. Laget, Nucl. Phys. A280, 405 (1977).

[5]A. Nagl and H. Überall, Phys. Lett. B 96, 254 (1980).

[6]V. DeCarlo *et al.*, Phys. Rev. C 21, 1460 (1980).

[7]A. N. Saharia and R. M. Woloshyn, Phys. Rev. C 23, 351 (1981).

[8]V. Devanathan, V. Girija, and G. N. Sivarama Prasad, Can. J. Phys. 58, 1151 (1980).

[9]A. Nagl and H. Überall, *Photopion Nuclear Physics* (Plenum, New York, 1979), p. 155.

[10]N. Freed, private communication; V. DeCarlo and N. Freed (unpublished).

[11]R. A. Meyer, W. B. Walters, and J. P. Hummel, Phys. Rev. B 138, 1421 (1965).

[12]F. A. Berends, A. Donnachie, and D. L. Weaver, Nucl. Phys. B 4, 1 (1967).

[13]G. F. Chew, M. L. Goldberger, F. E. Low, and Y. Nambu, Phys. Rev. 106, 1345 (1957).

[14]K. Stricker, H. McManus, and J. A. Carr, Phys. Rev. C 19, 929 (1979); 22, 2043 (1980).

[15]M. Krell and S. Barmo, Nucl. Phys. B 20, 461 (1970).

[16]V. Gillet and N. Vinh Mau, Nucl. Phys. 54, 321 (1964).

[17]M. Rho, Phys. Rev. Lett. 18, 671 (1967); Phys. Rev. 161, 955 (1967).

[18]L. S. Kisslinger, Lectures on Meson-Nucleus Physics, Orsay, report, 1973 (unpublished).

[19]M. E. Rose, Elementary Theory of Angular Momentum (Wiley, New York, 1957).

[20]B. D. Keister, Nucl. Phys. A350, 365 (1980).

[21]W. C. Haxton, Phys. Lett. 92, 37 (1980).

[22]V. Girija and V. Devanathan, Proc. Nucl. Phys. Solid State Phys. Symp. (India) 22B, 112 (1979).

[23]J. P. Albanese et al., Nucl. Phys. A350, 301 (1980).

[24]V. Devanathan, M. Rho, K. Srinivasa Rao, and S. C. K. Nair, Nucl. Phys. B2, 329 (1967).

[25]K. S. Rao and V. Devanathan, Can. J. Phys. 53, 1292 (1975).

[26]Ch. Schmitt and V. Walther, private communication. Besides the MIT and the Sendai groups, the experimental group at Mainz also proposes to study this reaction.